Short-Term Memory to Long-Term Memory Transition in a Nanoscale Memristor

Ting Chang, Sung-Hyun Jo, and Wei Lu*

Department of Electrical Engineering and Computer Science, University of Michigan, Michigan 48109, United States

ABSTRACT "Memory" is an essential building block in learning and decision-making in biological systems. Unlike modern semiconductor memory devices, needless to say, human memory is by no means eternal. Yet, forgetfulness is not always a disadvantage since it releases memory storage for more important or more frequently accessed pieces of information and is thought to be necessary for individuals to adapt to new environments. Eventually, only memories that are of significance are transformed from short-term memory into long-term memory through repeated stimulation. In this study, we show experimentally that the retention loss in a nanoscale memristor device bears striking resemblance to memory loss in biological systems. By stimulating the memristor with repeated voltage pulses, we observe an effect analogous to memory transition in biological systems with much improved retention time accompanied by additional structural changes in the memristor. We verify that not only the shape or the total number of stimuli is influential, but also the time interval between stimulation pulses (i.e., the stimulation rate) plays a crucial role in determining the effectiveness of the transition. The memory enhancement and transition of the memristor device was explained from the microscopic picture of impurity redistribution and can be qualitatively described by the same equations governing biological memories.

KEYWORDS: memristor · memory · retention · training · transition · neuromorphic system · synapse

A memristor[1−3] is a two-terminal device whose conductance can be modulated by external inputs with a memory effect due to internal state changes. Its concept[1] was first proposed 40 years ago and was recently linked to physical devices.[2] Like other nonlinear devices, a memristor is controlled by a (or a set of) internal state variable(s) which is in turn modulated by input signals. However, for a memristor the input signals at a given moment only determine the time derivative of the state variable, and the device state can be sufficiently determined only after knowing the history of the inputs. Mathematically, a memristor device is described by a set of equations that includes a current equation (eq 1) and a rate equation (eq 2):[3]

$$i = G(w, v)v \quad (1)$$

$$dw/dt = f(w, v) \quad (2)$$

Here G is the conductance linking the current and voltage, w is the internal state variable discussed above, and f is a function describing the change of w as a function of inputs and the current state. We note strictly speaking that eqs 1 and 2 describe a general class of memristive devices,[3] and here we use the term memristor to represent this general class of devices simply for the convenience of discussion without losing mathematical rigorousness. Despite its deceivingly simple two-terminal structure, a memristor can exhibit very complex behaviors when different terms are incorporated into the current equation and, in particular, the rate equation. For example, it has been concluded that all two-terminal nonvolatile memory devices based on resistive switching effects, that is, resistive random access memories (RRAM), are essentially memristors, regardless of materials or physical mechanisms utilized.[4]

The flexibility and generality of the memristor model allow the device to be used in a wide range of applications. As an example, RRAM has been studied as a leading candidate in nonvolatile memory applications[5] as a replacement for the flash memory technology due to attributes such as high density,[6,7] fast operation,[8,9] low power,[8] and CMOS compatibility.[9] Digital memory devices have been achieved in various material systems,[5,7,10,11] some of which also show multilevel switching,[8,9,12,13] allowing further increase of storage density. Recently, memristors have also been studied in biologically inspired neuromorphic circuits.[14−17] Important synaptic learning rules such as spike-timing dependent plasticity (STDP) have already been demonstrated.[15−17] However, to build successful artificial neural networks, a number of important synaptic functionalities remain to be achieved. One such example is

* Address correspondence to wluee@eecs.umich.edu.

Received for review August 5, 2011 and accepted August 23, 2011.

Published online August 23, 2011
10.1021/nn202983n

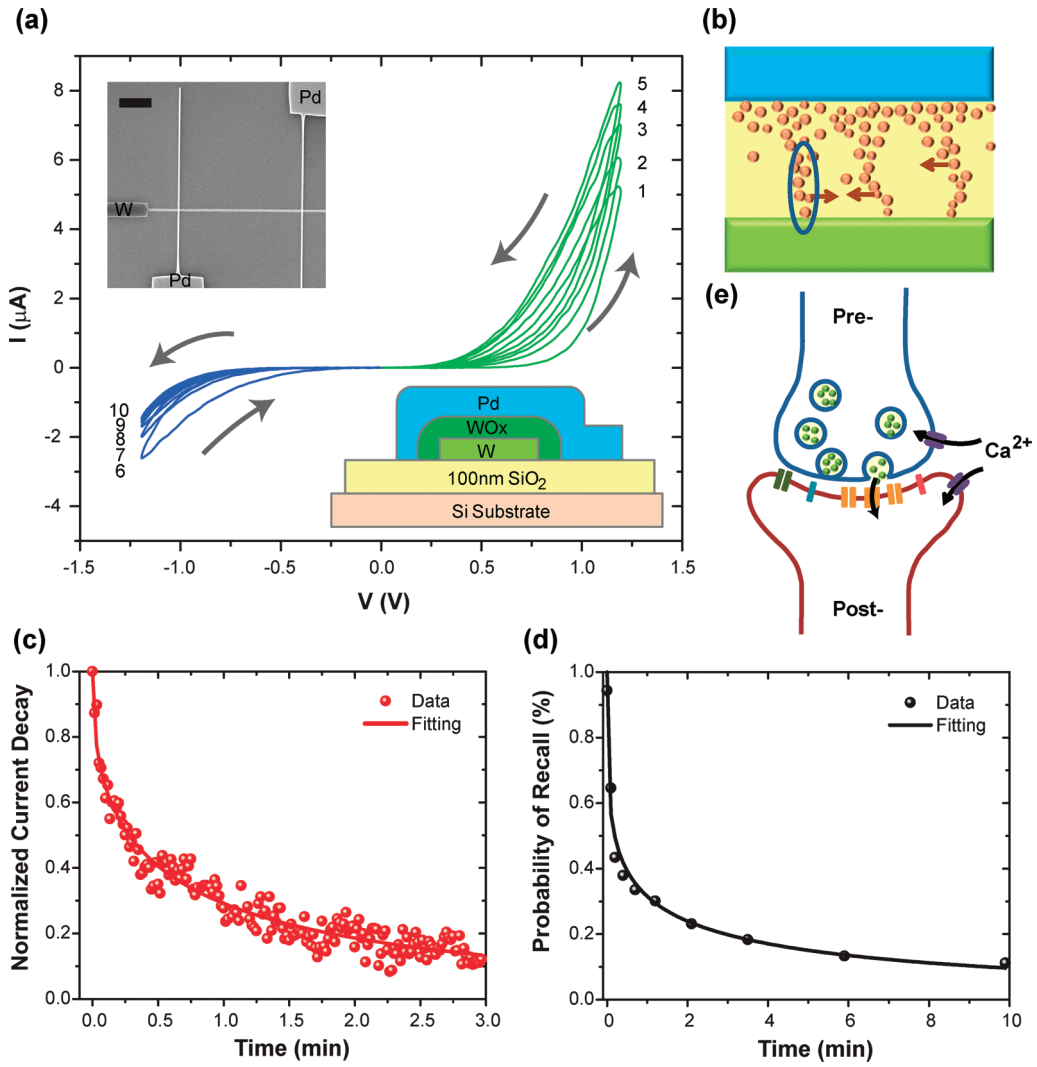

Figure 1. Memristor retention loss compared to memory loss. (a) DC *I*−*V* curves of a memristor studied here. Positive voltage sweeps (numbered 1−5, +1.2 V, 2 V/s) and negative voltage sweeps (numbered 6−10, −1.2 V, 2 V/s) increase and decrease the memristor conductance continuously, respectively. Overlap is seen on the positive side (green loops). The top and bottom insets are the SEM image of the memristor device (scale bar: 3 μm) and the cross section view of device structure, respectively. (b) Schematic illustration of oxygen vacancy diffusion in the memristor device. (c) A retention curve of the memristor. (d) A forgetting curve of human memory replicated and refitted from ref 28. (e) Schematic illustration of synaptic plasticity modulation between the axon (presynaptic) and the dendrite (postsynaptic).

"memory". Unlike modern semiconductor memory devices, needless to say, human memory is by no means eternal. Understanding how the memory is strengthened and transformed is an intensively studied field, and in numerous studies on biological systems it has been found that the rate of stimulation (*i.e.*, the time interval between stimulating pulses) plays a critical role.[18,19] Here we show that similar effects, including memory loss, memory transition, and the critical role of stimulation rate on the transition process, can be achieved in memristor devices. These demonstrations help pave the way of building bioinspired neuromorphic systems based on memristors.

RESULTS AND DISCUSSION

The memristor devices we study here are based on oxygen vacancy (V_{ox}) movement inside a WO_X thin-film.[20,21] In a previous work,[21] we have reported memristive effects obtained in such devices and presented a model based on eq 1 and eq 2 to describe the device behavior. Briefly, the memristive effects shown in Figure 1a are caused by the redistribution of oxygen vacancies near the WO_x/bottom-electrode interface. The oxygen vacancy-rich regions effectively form conducting channels as schematically illustrated in Figure 1b, and the device conductance can be increased or decreased by the creation or disruption of new parallel channels (or equivalently, changing the overall area of the conducting regions) by the movement of oxygen vacancies. More detailed discussions including quantitative modeling can be found in ref 21. In addition, by introducing a spontaneous diffusion term in addition to the field-assisted drift term to describe oxygen vacancy motion,[21] we can not only explain the

pinched-hysteresis loops but also account for the overlaps observed in the hysteresis loops, as evident in Figure 1a and also reported in other oxide-based memristors.[22] Qualitatively, the effect of diffusion can be explained with the aid of Figure 1b; when there are relatively few V_{ox} in the switching layer, the spontaneous, random motion of the V_{ox} can cause the conductive channels to be disrupted, and bring the device back to a less conductive state. Experimentally, this effect is reflected as loss of retention for the high-conductance state.

In the following, we show that the retention loss in the memristors bears remarkable similarities to memory loss in biological systems. Quantitatively, we find it suitable to model the spontaneous retention loss of the memristor by a stretched-exponential function (SEF)[23,24] which has been commonly used to describe electronic or structural relaxation in disordered materials such as glasses, polymers, or other dielectrics. For example, hydrogen diffusion in α-Si[25] and defect diffusion and hopping transport in complex condensed-matter systems[26] have been shown to agree well with this model. SEF, also known as the Kohlrausch law, is written as

$$\phi(t) = I_0 \exp[-(t/\tau)^{\beta}] \quad (3)$$

where $\phi(t)$ is the relaxation function, τ is the characteristic relaxation time, I_0 is the prefactor, and β is the stretch index ranging between 0 and 1. The stretched-exponential behavior originates from the wide distribution of activation energies and the associated wide range of relaxation times among different relaxation processes in a disordered system. Thus, τ and β in eq 3 jointly account for the collective behavior of all possible relaxation processes for V_{ox} in the memristor system.

Examining eq 3, one expects an abrupt drop when $t < \tau$, followed by a much slower decay when $t \gg \tau$. A brief description for human memory indeed coincides with this tendency, "a rapid initial decline is usually followed by a long, slow decay".[27] To further demonstrate the resemblance between the retention of the memristor and that of the human memory, we did the following test. We stimulated the memristor with short voltage pulses and recorded the retention data by reading the current with low voltage pulses every second for 3 min (Figure 1c, dots). The retention data are then fitted to SEF (Figure 1c, solid line). For comparison, Figure 1d shows the experimental data (dots) describing human memory loss[28] which are also fitted to SEF (solid line). Here, *probability of recall* is a measure of how successful a person can recall something remembered in the past after a period of time.

Neurobiologically, memory is thought to be closely associated with synaptic weights, the strength of synaptic connections.[29] A simple schematic of a synapse between a pre- and a postsynaptic neuron is shown in Figure 1e. Strengthening and weakening of synaptic weights are found to be governed by the concentrations of ionic species (*e.g.*, Ca^{2+}, Na^{+}, Mg^{2+}, and K^{+}) which activate/inhibit the release of neurotransmitters and receptors with certain timing constraints.[30,31] It can then be argued that memory decay involves a multitime constant relaxation process. Similar arguments can also be made by examining the memory trace network. If one views human memory trace as a chain consisting of numerous links, where one broken link leads to the failure of the entire chain and causes the memory to become inaccessible,[32] it is natural to describe the memory loss with the Weibull distribution, which is widely used for failure analysis (or equivalently, survival analysis). Mathematically, the cumulative Weibull distribution is just a complementary function of SEF (see Supporting Information). In fact, there have been examples[32,33] of psychologists characterizing memory retention with the *exponential-power function*, a synonym for SEF.

Undoubtedly, what mathematical function best portrays memory retention is a hot debate,[27] and the exact shape strongly depends upon the types of memory and experimental methods and is beyond the scope of this paper. However, if one assumes the simple picture that memory loss can be explained microscopically by the synaptic modifications with different time scales and macroscopically by the failure of memory trace networks, it is then perhaps not surprising that both memory loss and memristor retention loss can be described to first order by the same phenomenological equation (*e.g.*, eq 3).

In biological systems, short-term memory (STM) generally lasts from seconds to tens of minutes; on the contrary, long-term memory (LTM) lasts from a few hours to days or weeks, sometimes even to a lifetime.[35] Figure 2a shows a simplified illustration of the multistore memory model;[36] STM can only be sustained by constantly rehearsing the same stimulus, while LTM, despite the presence of natural forgetting, can be maintained for a much longer period of time without follow-up stimuli. The transition from STM to LTM is also through repetitions (as in rehearsal) but in this case, is a much more intricate process involving many molecular mechanisms and structural changes at various cellular sites/levels.[37] This entire, complicated process is termed consolidation[38] and will be discussed later. Below we show that a phenomenon similar to the STM-to-LTM transition can be achieved in a memristor upon repeated stimulations, with significant improvements in retention time ($\sim 20\times$) and a strong dependence on the time interval of the stimuli, analogous to the observed effects in biological systems.

The competing effect of memory loss and memory strengthening upon the application of stimuli is clearly observed in Figures 2b–d. In this study, we applied five consecutive stimulation voltage pulses

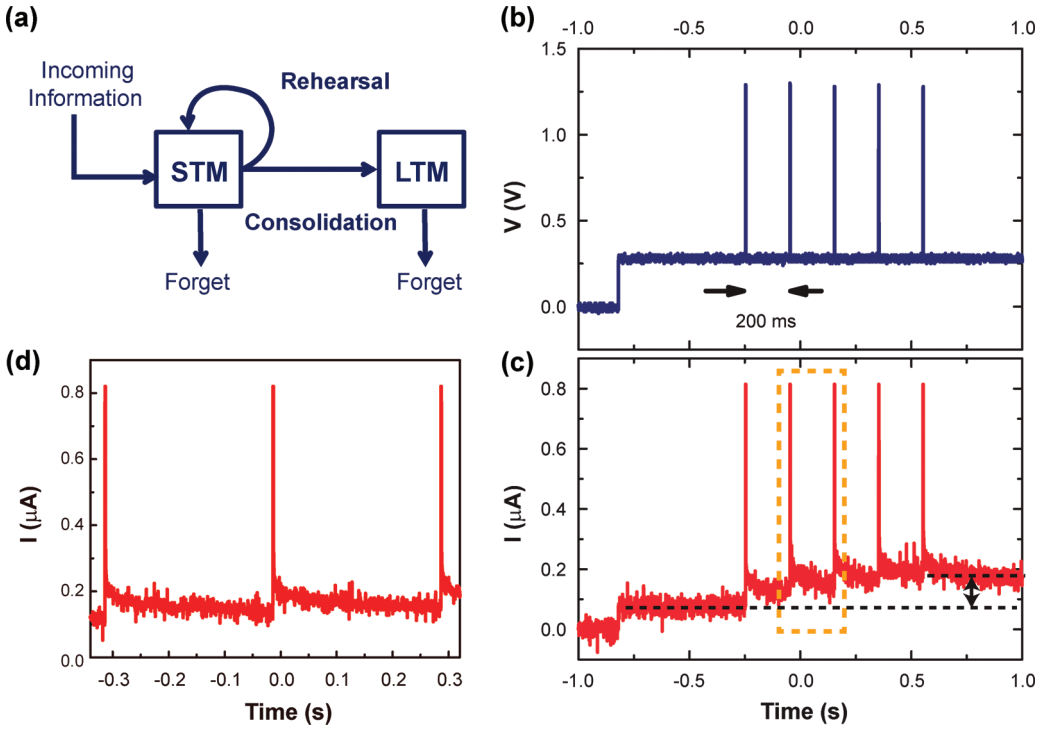

Figure 2. Memory enhancement with repeated stimulation. (a) Schematic of the multistore memory model. (b) The voltage profile applied to the memristor, consisting of five +1.3 V, 1 ms pulses and a constant +0.3 V read voltage. (c) The corresponding current through the memristor data recorded continuously throughout the test. The spontaneous decay after each pulse and the overall conductance enhancement can be observed. (d) A close-up view of the rectangular area in panel c highlighting the competing effects of memory enhancement and spontaneous decay.

(amplitude = +1.3 V, duration = 1 ms, period = 200 ms) and constantly monitored the memristor current, as shown in Figure 2b (see Methods). A low read voltage of 0.3 V was used to minimize disturbance on device conductance (Supporting Information Figure S1). Figure 2c shows that upon the application of each stimulation pulse, the device conductance is first enhanced, followed by a decay due to spontaneous diffusion discussed earlier. However, when the time interval between the stimulation is relatively short, (*e.g.*, 199 ms in Figure 2b), an overall increase of the memristor conductance can be observed despite the spontaneous decay (Figures 2c and 2d). This is because the idle time between the stimulation pulses is not long enough for the memristor to relax to its initial state, resulting in a net conductance increase. We note this observation is akin to well-studied biological processes—paired-pulse facilitation (PPF)[18] and post-tetanic potentiation (PTP).[19] More discussions on the effects of stimulation rate will be provided later.

Interestingly, not only is the amplitude of the memristor conductance improved upon repeated stimulation, the retention time also improves significantly with stimulation. To verify this effect, we applied stimuli of identical voltage pulses with fixed height, width, and pulse-to-pulse interval (see Methods). Different numbers of stimulations ($N = 5$ to $N = 40$ in steps of 5) were applied to the same memristor device starting from the same initial state, and retention curves were recorded right after the last stimuli in each stimulation series. Figure 3a shows results obtained from tests after 5, 10, ..., 35, and 40 stimuli, along with fittings using eq 3. Both the retention time (represented as τ in eq 3) and the synaptic weight (represented as I_0 in eq 3) can then be obtained from the fitting. Figure 3b shows the retention time (τ) plotted with respect to the number of stimulations (N). An obvious improvement of τ with repetitive stimulation can be observed. Overall, τ is increased by approximately 20-fold and slightly saturates beyond 20 repetitions. As a result, it seems natural to suggest two memory regimes exist in the memristor device, consisting of a regime with short $\tau \approx$ few seconds and sensitive to additional stimulations, and another regime with much longer $\tau \approx$ minutes and relatively insensitive to additional stimulations. Also plotted in Figure 3b is the synaptic weight (I_0) . A similar trend can be found for τ and I_0 with increasing N. The two memory regimes and the transition between them in the memristor device can be schematically explained with the aid of Figure 3c. With the addition of repeated stimulation, a higher concentration of V_{ox} is moved into the switching layer, and the lateral diffusion of V_{ox} eventually balances each other out and has a much lower probability to break the conducting paths, and as a result the retention time improves along with the memristor conductance until the time when significant V_{ox} is stored and the retention time and the conductance saturates. We note similar effects

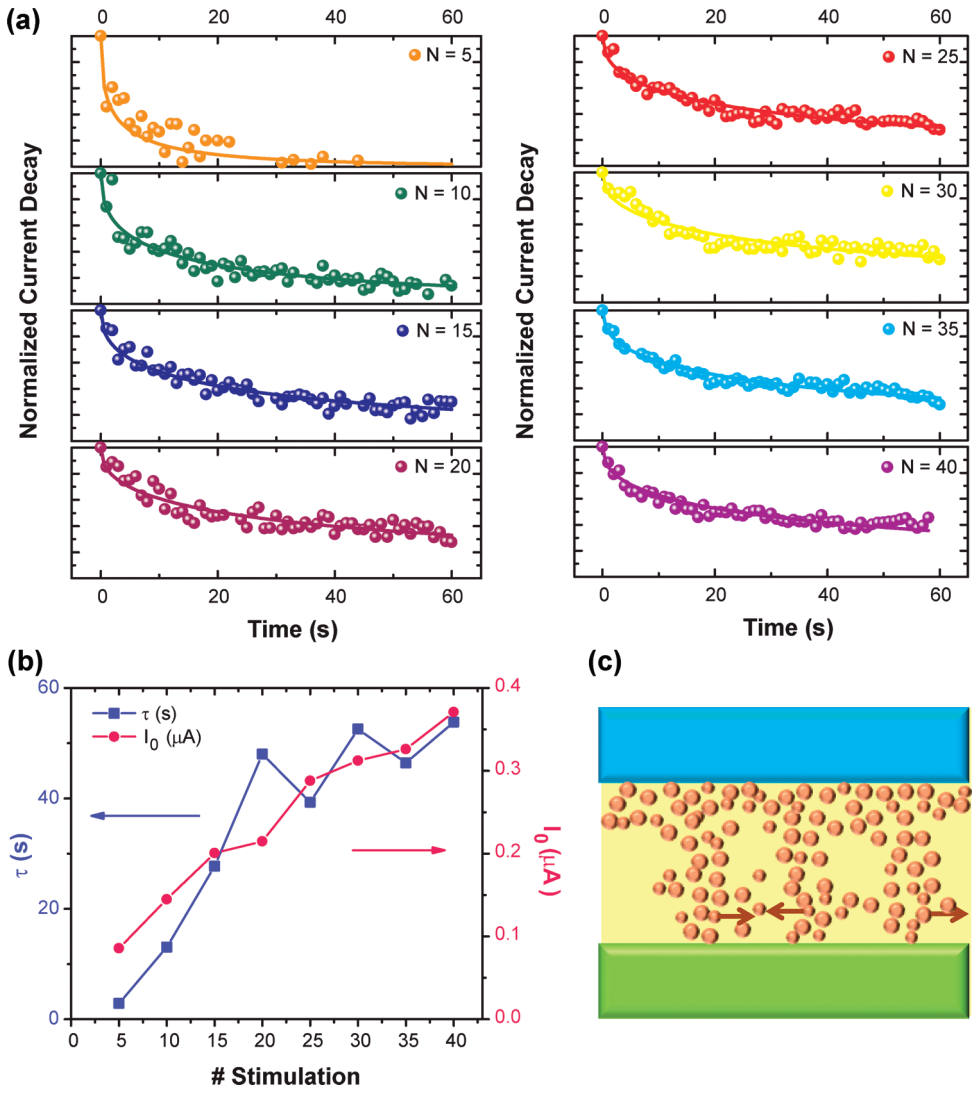

Figure 3. STM-to-LTM transition. (a) Memory retention data recorded after different numbers of identical stimuli (dots) and fitted curves using the SEF (solid lines). The data are scaled by a prefactor I_0. (b) Characteristic relaxation time (τ) obtained through the fitting in panel a and the prefactor (I_0) plotted with respect to the number of stimulations (N). (c) Schematic of the structural change to the memristor corresponding to the improved retention. After repeated stimulation, there are sufficient V_{ox} in the switching layer that lateral diffusion effectively cancels out, resulting in much improved retention along with the increase in conductance (synaptic weight).

are well-known in the STM-to-LTM transition in biological systems.[35,37] Formation, stabilization, and persistence of LTM are supported by experimental evidence of the growth of new synaptic connections and dendrite size/shape change, adding more pathways for synaptic transmission. LTM still fades with time, indicating that synaptic connections retract with time, but at a much slower pace than the decay during STM. Considering these similarities, we argue that the key attributes of the STM-to-LTM transition process have been demonstrated in the memristor device including the significant increase in memory retention after repeated stimulation and the resulting structural change, as discussed above.

We further investigated in detail how different stimulation conditions affect the outcome of the memory transition. It is obvious that pulse amplitude and duration are important factors that can affect the transition (Supporting Information, Figure S2). However, a less obvious but biologically important effect is that the transition is strongly dependent on the stimulation rate (equivalently, time interval between stimulation pulses) (Supporting Information, Figure S3).[18,19] To examine the effect of stimulation rate on the memristor, we again used identical pulses as stimuli but fixed the number of stimulation at $N = 10$ and varied only the interval between stimuli (Δt), from as short as 15 ms to as long as 10 s (see Methods). This configuration ensures that the total flux (*e.g.*, time integral of the applied voltage) applied to the memristor remains fixed, with the only varying parameter being the stimulation rate.

Figure 4a shows the response of the memristor to different stimulation rates. Here the memristor

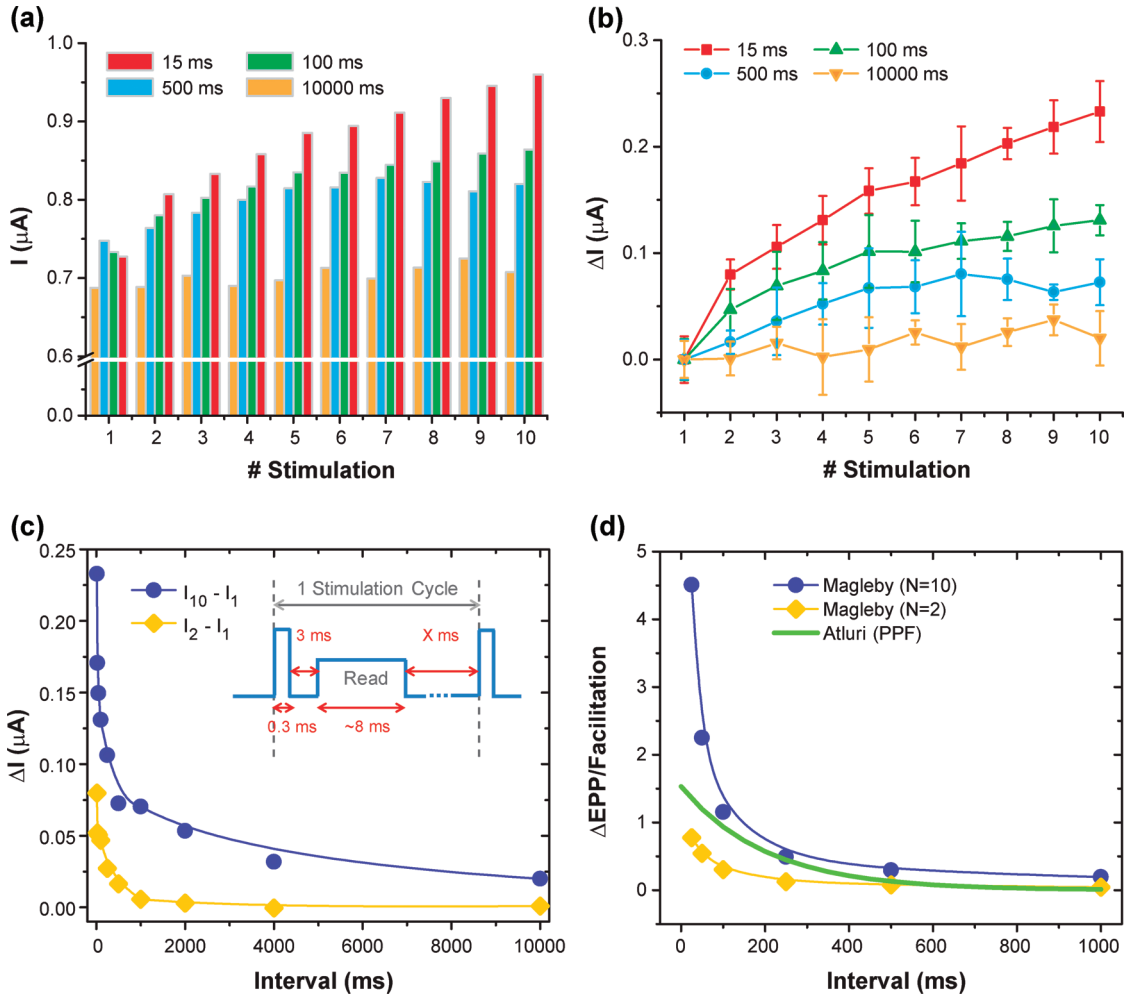

Figure 4. Dependence of the transition efficiency on stimulation rate. (a) Current through the memristor recorded after each stimulation pulse, at different pulse interval conditions. (b) Current increase (ΔI) after every stimulus plotted against pulse number for different pulse interval conditions. Each measurement was repeated five times. Solid marks and error bars represent the mean and standard deviation (SD), respectively. (c) Extracted $I_2 - I_1$ and $I_{10} - I_1$, representing PPF and PTP, *versus* the interval of the stimulation pulses (in milliseconds). Inset shows the voltage profile used for this measurement. The lines are simply guides to the eyes. (d) Similar effects on stimulation rates observed in biological systems, showing data for PPF (green lines, adapted from ref 18 and yellow diamonds, calculated using the approach provided in ref 38) and PTP (blue dots, calculated using the approach provided in ref 38).

conductance (represented by the current of I_1, I_2, ..., I_{10} read at low voltage) was recorded immediately after each stimulation pulse, and different pulsing conditions are represented by different colors and symbols. For Δt = 10 s, barely any increase in current is seen, whereas for Δt = 15 ms, the upward trend is apparent. This effect is more clearly illustrated in Figure 4b, where we plot the current increase (ΔI) for different pulsing conditions. Here ΔI is calculated by offsetting the current (I_N, N = 1, 2, ..., 10) by I_1. The measurements were repeated five times to minimize fluctuations in data, with solid marks and error bars in Figure 4b representing the mean and standard deviation, respectively. A clear dependence of the conductance enhancement on the stimulation rate can be observed in Figure 4b, with a high stimulation rate being the most effective and low stimulation rate being the least effective. To quantify the conductance enhancement, we plot ($I_2 - I_1$) and ($I_{10} - I_1$), which represent, respectively, the experimental conditions for PPF and PTP used in biological studies, for each interval condition in Figure 4c. For comparison in Figure 4d we plot similar rate-dependent effects observed in biological systems. For PPF,[18] it was found that in the granule/Purkinje cell synapse there is an elevation in responsiveness for the second pulse when two pulses are less than 1 s apart, as illustrated by the green curve in Figure 4d. Similarly, studies on frog neuromuscular junctions showed that the magnitude of facilitation after repetitive stimulation (N = 2, corresponding to PPF and plotted as the yellow curve; or N = 10, corresponding to PTP and plotted as the blue curve)[19,38] also exhibits a strong dependence on the stimulation interval (see Methods). The reason for the rate dependence in biological systems can be briefly explained as the following. A stimulus (action potential) at the

presynaptic neuron permits calcium influx that initiates the release of neurotransmitters, thereby temporarily enhancing synaptic transmission. Once the stimulus is terminated, it requires a finite time for the residual Ca^{2+} to decay to its equilibrium level. Hence, if another identical stimulus succeeds shortly after this stimulus, the response of the synapse will be enhanced, as in PPF. In the same fashion, if many stimuli follow closely one after another, synaptic transmission will progressively grow with the increasing number of stimuli, as in PTP. In the memristor device, similar competing effects exist between the stimulation pulses and the diffusion of V_{ox}, and lead to the similar rate dependence observations. These comparisons again verify the feasibility of using memristors to emulate memory transitions for neuromorphic systems.

CONCLUSION

In summary, we have successfully demonstrated an effect analogous to STM-to-LTM transition in a nanoscale memristor device. The pronounced similarity between ion diffusion and memory decay is explained by the stretched-exponential relaxation that reasonably correlates physical mechanisms to both phenomena. We showed that the memristor device retention can be improved with the application of repeated stimulations in a fashion similar to the STM-to-LTM transition in biological systems. In addition, we verified that not only the shape or the total number of stimuli is influential, but also the interval between repetitions also plays an important role in determining the effectiveness of the STM-to-LTM transition. Considering memory is an essential building block in learning and decision-making, the demonstration of such functionalities in a nanoscale memristor synapse is crucial for the realization of neuromorphic systems and artificial neural networks.

More strictly, memory consolidation in biological systems is a complex process comprising synaptic consolidation, system consolidation, and reconsolidation.[39] The most important physiological mechanism underlying synaptic consolidation is long-term potentiation (LTP) by which strong and long-lasting synaptic connections are formed.[40] Whereas synaptic consolidation takes place from minutes to hours after a learning or stimulation event, system consolidation occurs days to weeks after the event, and during this period of time brain circuits are reorganized so that memories become stable within the system. However, memories become labile and unstable after recalls, and reconsolidation is necessary to stabilize, modify, and strengthen LTM. Oftentimes, the formation of STM (rehearsal) and LTM (consolidation) involves not only molecular and cellular reactions, but also cognitive and psychological behaviors.[41,42] Whether in neurobiology or in psychology, details of these processes are still under debate. Hence, we would like to emphasize that our objective of this study is to demonstrate phenomena observed in a memristor synapse that exhibit similar effects to the STM-to-LTM transition in biological systems, instead of trying to form strict one-to-one correlation with biological systems at the molecular or cellular level.

METHODS

Device Fabrication. The memristor device consists of a W bottom electrode, a Pd top electrode, and a WO_X film sandwiched in between. Tungsten oxide is formed by rapid thermal annealing (RTA) at 400 °C. All lithography steps are performed with electron-beam (Raith 150), and the dimension of the junction is approximately 130 nm × 130 nm. A scanning electron microscope (SEM) image and a cross-section schematic of the device are shown in the insets of Figure 1a.

Measurement and Analysis. To obtain the data in Figure 2, we applied stimulation pulses to the top electrode of the memristor through an arbitrary function generator (Tektronix AFG3101). The current was measured with a current preamplifier, and the data were captured with an oscilloscope (Tektronix TDS 3032B) with the bottom electrode grounded. The applied signal is shown in Figure 2b and includes a constant read voltage of 0.3 V and five voltage pulses (amplitude = +1.3 V, duration = 1 ms, period = 200 ms). Pulses with periods of 100 and 300 ms are also used, and the results are shown in Supporting Information, Figure S3.

To obtain the STM-to-LTM transition data in Figure 3, repeated stimulation pulses (amplitude = +1.3 V, duration = 0.4 ms, pulses interval = 60 ms) were applied to the memristor. Retention curves were obtained by reading the current every second with +0.5 V, 8 ms read pulses immediately after the last stimulus in the series. This measurement was performed with custom-built LabWindows/CVI programs. All retention curves were then normalized by their own prefactor (I_0), which is the difference in current right before and right after the series of stimuli in each case. The normalized retention curves were then fitted with eq 3 with a fixed $\beta = 0.45$, keeping τ as the only fitting parameter for each case. β is a material-dependent parameter, thus it is reasonable to assume β as a constant in the same device under normal operations.

To obtain the rate-dependent transition experiment results in Figure 4, we fixed the number of stimulation and the shape of the stimulation pulses, and only varied the stimulation interval. The interval being tested were 15 ms, 25 ms, 50 ms, 100 ms, 250 ms, 500 ms, 1 s, 2 s, 4 s, and 10 s; +1.3 V, 0.3 ms voltage pulses were applied as stimuli. A +0.5 V, 8 ms read pulse followed each stimulus pulse by a 3 ms delay. The voltage profile is shown in the inset of Figure 4c.

The green curve in Figure 4d was adapted from an exponential decay function of PPF between the granule/Purkinje cell synapse,[18] where the amplitude and the time constant were 153% and 203 ms, respectively. This curve describes how much the response to the second pulse is facilitated comparing to the first pulse with respect to the pulse-to-pulse interval. The blue and yellow marks in Figure 4d were calculated using the model in ref 38 using scheme II, and all the parameters used in the calculation were obtained from the legend of Figure 4 in the same reference.

Acknowledgment. This work was partially supported in part by the DARPA SyNAPSE program under Contract HRL0011-09-C-001 and by an NSF CAREER award ECCS-0954621. This work used the Lurie Nanofabrication Facility at the University of Michigan, a member of the National Nanotechnology Infrastructure Network (NNIN) funded by NSF.

Supporting Information Available: Derivation of the stretched-exponential function from the Weibull distribution and effects of the stimulation pulse height, width, and interval on the retention time. This material is available free of charge *via* the Internet at http://pubs.acs.org.

REFERENCES AND NOTES

1. Chua, L. O. Memristor—The Missing Circuit Element. *IEEE Trans. Circuit Theory* **1971**, *18*, 507–519.
2. Strukov, D. B.; Snider, G. S.; Stewart, D. R.; Williams, R. S. The Missing Memristor Found. *Nature* **2008**, *453*, 80–83.
3. Chua, L. O.; Kang, S. M. Memristive Devices and Systems. *Proc. IEEE* **1976**, *64*, 209–223.
4. Chua, L. Resistance Switching Memories Are Memristors. *Appl. Phys. A: Mater. Sci. Process.* **2011**, *102*, 765–783.
5. Waser, R.; Aono, M. Nanoionics-Based Resistive Switching Memories. *Nat. Mater.* **2007**, *6*, 833–840.
6. Jung, G. Y.; Johnston-Halperin, E.; Wu, W.; Yu, Z.; Wang, S. Y.; Tong, W. M.; Li, Z.; Green, J. E.; Sheriff, B. A.; Boukai, A.; *et al.* Circuit Fabrication at 17 nm Half-Pitch by Nanoimprint Lithography. *Nano Lett.* **2006**, *6*, 351–354.
7. Jo, S. H.; Kim, K. H.; Lu, W. High-Density Crossbar Arrays Based on a Si Memristive System. *Nano Lett.* **2009**, *9*, 870–874.
8. Lee, H. Y.; Chen, P. S.; Wu, T. Y.; Chen, Y. S.; Wang, C. C.; Tzeng, P. J.; Lin, C. H.; Chen, F.; Lien, C. H.; Tsai, M. J. Low Power and High Speed Bipolar Switching with a Thin Reactive Ti Buffer Layer in Robust HfO_2 Based RRAM. *Tech. Dig., Int. Elect. Dev. Meet.* **2008**, 297–300.
9. Jo, S. H.; Lu, W. CMOS Compatible Nanoscale Nonvolatile Resistance Switching Memory. *Nano Lett.* **2008**, *8*, 392–397.
10. Cario, L.; Vaju, C.; Corraze, B.; Guiot, V.; Janod, E. Electric-Field-Induced Resistive Switching in a Family of Mott Insulators: Towards a New Class of RRAM Memories. *Adv. Mater.* **2010**, *22*, 5193–5197.
11. Jeong, H. Y.; Kim, J. Y.; Kim, J. W.; Hwang, J. O.; Kim, J. E.; Lee, J. Y.; Yoon, T. H.; Cho, B. J.; Kim, S. O.; Ruoff, R. S.; *et al.* Graphene Oxide Thin Films for Flexible Nonvolatile Memory Applications. *Nano Lett.* **2010**, *10*, 4381–4386.
12. Yoshida, C.; Tsunoda, K.; Noshiro, H.; Sugiyama, Y. High Speed Resistive Switching in $Pt/TiO_2/TiN$ Film for Nonvolatile Memory Application. *Appl. Phys. Lett.* **2007**, *91*, 223510.
13. Wang, S. Y.; Huang, C. W.; Lee, D. Y.; Tseng, T. Y.; Chang, T. C. Multilevel Resistive Switching in $Ti/Cu_XO/Pt$ Memory Devices. *J. Appl. Phys.* **2010**, *108*, 114110.
14. Snider, G. S. Spike-Timing Dependent Learning in Memristive Nanodevices. *IEEE/ACM Int. Symp. Nanoscale Architectures* **2008**, 85–92.
15. Jo, S. H.; Chang, T.; Ebong, I.; Bhadviya, B. B.; Mazumder, P.; Lu, W. Nanoscale Memristor Device as Synapse in Neuromorphic Systems. *Nano Lett.* **2010**, *10*, 1297–1301.
16. Alibart, F.; Pleutin, S.; Guérin, D.; Novembre, C.; Lenfant, S.; Lmimouni, K.; Gamrat, C.; Vuillaume, D. An Organic Nanoparticle Transistor Behaving as a Biological Spiking Synapse. *Adv. Funct. Mater.* **2010**, *20*, 330–337.
17. Hesegawa, T.; Ohno, T.; Terabe, K.; Tsuruoka, T.; Nakayama, T.; Gimzewski, J. K.; Aono, M. Learning Abilities Achieved by Single Solid-State Atomic Switch. *Adv. Mater.* **2010**, *22*, 1–4.
18. Atluri, P. P.; Regehr, W. G. Determinants of the Time Course of Facilitation at the Granule Cell to Purkinje Cell Synapse. *J. Neurosci.* **1996**, *16*, 5661–5671.
19. Magleby, K. L. The Effect of Repetitive Stimulation on Facilitation of Transmitter Release at the Frog Neuromuscular Junction. *J. Physiol.* **1973**, *234*, 327–352.
20. Yang, J. J.; Pickett, M. D.; Li, X.; Ohlberg, D. A. A.; Stewart, D. R.; Williams, R. S. Memristive Switching Mechanisms for Metal/Oxide/Metal Nanodevices. *Nat. Nanotechnol.* **2008**, *3*, 429–433.
21. Chang, T.; Jo, S. H.; Kim, K. H.; Sheridan, P.; Gaba, S.; Lu, W. Synaptic Behaviors and Modeling of a Metal Oxide Memristive Device. *Appl. Phys. A: Mater. Sci. Process.* **2011**, *102*, 857–863.
22. Li, H.; Xia, Y.; Xu, B.; Guo, H.; Yin, J.; Liu, Z. Memristive Behaviors in $LiNbO_3$ Ferroelectric Diodes. *Appl. Phys. Lett.* **2010**, *97*, 012902.
23. Scher, H.; Shlesinger, M. F.; Bendler, J. T. Time-Scale Invariance in Transport and Relaxation. *Phys. Today* **1991**, *44*, 26–34.
24. Phillips, J. C. Stretched Exponential Relaxation in Molecular and Electronic Glasses. *Rep. Prog. Phys.* **1996**, *59*, 1133–1207.
25. Kakalios, J.; Street, R. A.; Jackson, W. B. Stretched-Exponential Relaxation Arising from Dispersive Diffusion of Hydrogen in Amorphous Silicon. *Phys. Rev. Lett.* **1987**, *59*, 1037–1040.
26. Sturman, B.; Podivilov, E.; Gorkunov, M. Origin of Stretched Exponential Relaxation for Hopping-Transport Models. *Phys. Rev. Lett.* **2003**, *91*, 176602.
27. Wixted, J. T.; Ebbesen, E. B. On the Form of Forgetting. *Psychol. Sci.* **1991**, *2*, 409–415.
28. Rubin, D. C.; Hinton, S.; Wenzel, A. The Precise Time Course of Retention. *J. Exp. Psychol. Learn.* **1999**, *25*, 1161–1176.
29. Grimwood, P. D.; Martin, S. J.; Morris, R. G. M. Synaptic Plasticity and Memory. In *Synapses*; Cowan, W. M., Ed.; Johns Hopkins University Press: Baltimore, MD, 2001; p 519.
30. Bi, G. Q.; Poo, M. M. Synaptic Modifications in Cultured Hippocampal Neurons: Dependence on Spike Timing, Synaptic Strength, and Postsynaptic Cell Type. *J. Neurosci.* **1998**, *2*, 10464–10472.
31. Zucker, R. S.; Regehr, W. G. Short-Term Synaptic Plasticity. *Annu. Rev. Physiol.* **2002**, *64*, 355–405.
32. Rubin, D. C.; Wenzel, A. E. One Hundred Years of Forgetting: A Quantitative Description of Retention. *Psychol. Rev.* **1996**, *103*, 734–760.
33. Wickelgren, W. A. *J. Math.* Trace Resistance and the Decay of Long-Term Memory. *Psychol.* **1972**, *9*, 418–455.
34. Kandel, E. R. The Molecular Biology of Memory Storage: a Dialogue between Genes and Synapses. *Science* **2001**, *294*, 1030–1038.
35. Shiffrin, R. M.; Atkinson, R. C. *Psycho.* Storage and Retrieval Processes in Long-Term Memory. *Rev.* **1969**, *76*, 179–193.
36. Lamprecht, R.; LeDoux, J. Structural Plasticity and Memory. *Nat. Rev. Neurosci.* **2004**, *5*, 45–54.
37. McGaugh, J. L. Memory—A Century of Consolidation. *Science* **2000**, *287*, 248–251.
38. Magleby, L. K.; Zengel, J. E. A Quantitative Description of Stimulation-Induced Changes in Transmitter Release at the Frog Neuromuscular Junction. *J. Gen. Physiol.* **1982**, *80*, 613–638.
39. Dudai, Y. The Neurobiology of Consolidations, or, How Stable Is the Engram? *Annu. Rev. Psychol.* **2004**, *55*, 51–86.
40. Bliss, T. V. P.; Collingridge, G. L. A Synaptic Model of Memory: Long-Term Potentiation in the Hippocampus. *Nature* **1993**, *361*, 31–39.
41. Roediger III, H. L.; Weinstein, Y.; Agarwal, P. K. Forgetting: Preliminary Considerations. In *Forgetting*; Sala, S. D., Ed.; Psychology Press: New York, 2010; p 1.
42. Sweatt, J. D. *Mechanisms of Memory*, 2nd ed.; Academic: Amsterdam, The Netherlands, 2010.